Journal of the Serbian Society for Computational Mechanics / Vol. 19 / No. 1, 2025 / pp 115-124 / review paper
(10.24874/jsscm.2025.19.01.04)

VARIOUS FINITE ELEMENTS IN NUMERICAL ANALYSIS OF UNIAXIAL TESTS FOR THE CONCRETE DAMAGED PLASTICITY (CDP) CONSTITUTIVE MODEL

Vladimir Dunić[1*] [0000-0003-1648-1745], Nenad Grujović[1] [0000-0002-8765-2196], Aleksandar Bodić[1] [0000-0002-1713-6540], Dragan Rakić[1] [0000-0001-5152-5788], Miroslav Živković[1] [0000-0002-0752-6289]

[1] University of Kragujevac, Faculty of Engineering, Kragujevac, Serbia
e-mail: dunic@kg.ac.rs
**corresponding author*

Abstract

The concrete damaged plasticity (CDP) model is one of the most popular constitutive models implemented into various Finite Element Method software. The application to the real structures is documented in the literature, but still there are some doubts about the response in combination with the various finite elements. Simple benchmark examples simulated by the PAK software are used to show the open questions and possible answers. Testing of tetrahedral and hexahedral finite elements, as well as the various time increment provided the discussion and conclusions which can be useful for further simulations of real concrete structures' response.

Keywords: Concrete damaged plasticity, tetrahedral and hexahedral finite elements, Constitutive model, Finite element method, PAK software

1. Introduction

Various constitutive models have been developed for a nonlinear analysis of concrete structures. These models are most often based on a theory of plasticity, a continuum damage mechanics theory or their combination. Concrete damage plasticity (CDP) material model is a constitutive model used for the analysis of concrete structures subjected to static or dynamic loads and is based on a combination of the theory of plasticity and the damage mechanics theory (Grassel et al. 2013).

Many papers can be found in the literature related to the application of the CDP material model for solving various problems such as reinforced concrete structures (Szczecina and Winnicki 2015; Wang et al. 2020), structures subjected to blast loading (Talaat et al. 2021), structures subjected to impact loading (Fedoroff and Calonius 2020; Martin 2010), concrete structures subjected to high strain-rate loadings (Altaee et al. 2020), green concrete mixture modelling (Bosro et al. 2024) etc. CDP model usage for simulating the behavior of high-strength concrete under static and dynamic loading conditions is described in (Le Minh et al. 2021). Input parameters optimization for the CDP model is given in (Labibzadeh et al. 2017) along with a procedure for obtaining a unique set of parameters for reinforced concrete slab. A parameter

sensitivity for this constitutive model is investigated in (Qasem et al. 2025) where the authors optimized and calibrated CDP model with improved accuracy in simulating a concrete behavior. The effect of size on the performance of the CDP model was investigated in (Labibzadeh and Namjoo 2020). They showed that the CDP model, with a unique set of input parameters, accurately predicts beam behavior regardless of size. The description of damage behavior and the procedure for assessing damage in a concrete was investigated in (Al-Zuhairi et al. 2022; Sümer and Aktaş 2015). It can be used for simulating concrete behavior in a damaged plasticity model accurately. Our previous research (Rakić et al. 2021) showed a complete procedure for the identification of material parameters for the CDP model.

This paper examines the influence of the type of finite elements on the results of numerical simulations using the CDP model. In the CDP model, the concrete structures' response is controlled by the yield function originally developed by (Lubliner et al. 1989), and later improved by (Lee and Fenves 1998). Numerical analyses are conducted for the different types of finite elements: hexahedral with and without midside nodes, tetrahedral with and without midside nodes and hexahedral finite element degenerated into tetrahedron shape. The simulations were performed in PAK software (Kojić et al. 1999).

In section 2, the theoretical basis related to the CDP material model is given. Section 3 gives the description of FE models for the uniaxial compressive and tensile tests, the finite element type used for numerical simulations, the boundary conditions and loads. Section 4 compares the results of the numerical simulations for the various types of finite elements in the form of stress-total strain dependencies and discusses the obtained results. At the end of the paper, conclusions are given about the conducted analyzes as well as directions for the future research in this area.

2. Concrete damaged plasticity constitutive model

The CDP model is well known and documented in the literature, but here the main relations will be considered as it is implemented into the PAK software. As it is common for many constitutive models which are used for simulation of material nonlinear behavior, the total strain can be additively decomposed into the elastic and the plastic strain component (Kojić et al. 1998; Kojić and Bathe 2005):

$$\mathbf{e} = \mathbf{e}^E + \mathbf{e}^P . \tag{18}$$

The elastic part is a recoverable part of the total strain, which defines the effective (undamaged) stress tensor as (Lee 1996):

$$\bar{\boldsymbol{\sigma}} = \mathbf{D}_0 : \mathbf{e}^E \ , \tag{19}$$

where $\mathbf{D}_0$ denotes the undamaged elastic stiffness tensor. From equations (1) and (2), the stress can be computed as follows:

$$\bar{\boldsymbol{\sigma}} = \mathbf{D}_0 : \left(\mathbf{e} - \mathbf{e}^P\right). \tag{20}$$

Because the maximal eigen stress is necessary for the computation of yield function, the diagonal eigen stress tensor is transformed as:

$$\hat{\bar{\boldsymbol{\sigma}}}^{tr} = \mathbf{P}^{-1}\bar{\boldsymbol{\sigma}}^{tr}\mathbf{P}^{-T} , \tag{21}$$

where $\mathbf{P}$ is the transformation matrix $\bar{\boldsymbol{\sigma}}^{tr}$. In the equilibrium iterations, the constitutive matrix used is the damaged elastic stiffness matrix, expressed as $(1-d)\mathbf{D}_0$. In other words, the elastic

stiffness matrix is scaled by the scalar degradation variable $(1-d)$, so that the reduction of stiffness due to material degradation is directly accounted for. Now, it is possible to calculate the yield function of CDP constitutive model by equation (Lee 1996; Rakić et al. 2021):

$$F(\hat{\bar{\boldsymbol{\sigma}}}^{tr},\boldsymbol{\kappa})=\frac{1}{1-\alpha}\left(\alpha\left(\hat{\bar{I}}_1^{tr}\right)+\sqrt{\frac{3}{2}}\left\|\hat{\bar{\mathbf{S}}}^{tr}\right\|+\beta(\boldsymbol{\kappa})\left\langle\left(\hat{\bar{\sigma}}_1^{tr}\right)\right\rangle\right)-\bar{\sigma}_c(\boldsymbol{\kappa}) \tag{22}$$

where, $\boldsymbol{\kappa}=\left[\kappa_c,\kappa_t\right]$ is the damage vector which consist of compression and tension component, $\bar{\sigma}_c(\boldsymbol{\kappa})$ is the material cohesion, $\hat{\bar{I}}_1^{tr}=\mathrm{tr}\hat{\bar{\boldsymbol{\sigma}}}^{tr}$ is the first stress tensor invariant, $\left\|\hat{\bar{\mathbf{S}}}^{tr}\right\|=\sqrt{\hat{\bar{\mathbf{S}}}^{tr}:\hat{\bar{\mathbf{S}}}^{tr}}$ is the stress tensor deviator norm, $\hat{\bar{\mathbf{S}}}^{tr}=\hat{\bar{\boldsymbol{\sigma}}}^{tr}-\hat{\bar{\sigma}}_m\mathbf{I}$ is the deviator of effective stress, $\hat{\bar{\sigma}}_m=\frac{1}{3}\mathrm{tr}\hat{\bar{\boldsymbol{\sigma}}}^{tr}$ is the mean effective stress, and $\hat{\bar{\sigma}}_1^{tr}$ is the algebraic maximum of eigenvalues of effective stress tensor. In the case when $F(\hat{\bar{\boldsymbol{\sigma}}}^{tr},\boldsymbol{\kappa})<0$, the solution is elastic and there is no damage or plastic strain increase. However, if the condition is not satisfied, the stress integration procedure is employed. Firstly, the parameter should be calculated at the integration point level:

$$\Delta\lambda=\frac{\alpha\left(\hat{\bar{I}}_1^{tr}\right)+\sqrt{\frac{3}{2}}\left\|\hat{\bar{\mathbf{S}}}^{tr}\right\|+\beta\left(\hat{\bar{\sigma}}_1^{tr}\right)-(1-\alpha)\bar{\sigma}_c}{9K_0\alpha_p\alpha+\sqrt{6}G_0+\beta\left[2G_0\dfrac{\left(\hat{\bar{S}}_1^{tr}\right)}{\left\|\hat{\bar{\mathbf{S}}}^{tr}\right\|}+3K_0\alpha_p\right]} \tag{23}$$

where α and β are biaxial loading parameters, K_0 is the compressibility modulus, α_p is the dilatancy, while G_0 is the shear modulus. Now, it is possible to update the stress tensor as follows:

$$\hat{\bar{\boldsymbol{\sigma}}}=\hat{\bar{\boldsymbol{\sigma}}}^{tr}-\Delta\lambda\left[2G_0\frac{\hat{\bar{\mathbf{S}}}^{tr}}{\left\|\hat{\bar{\mathbf{S}}}^{tr}\right\|}+3K_0\alpha_p\mathbf{I}\right] \tag{24}$$

The damage equation and the residual of damage are

$$\mathbf{Q}=-\Delta\boldsymbol{\kappa}+\Delta\lambda\mathbf{H} \tag{25}$$

where $\mathbf{H}$ is the matrix which takes into account both tension and compression influence. If the condition $\|\mathbf{Q}\|=\sqrt{\mathbf{Q}:\mathbf{Q}}<tol$ is satisfied, the damage vector remains unchanged and further update of the plastic strain, degradation and strain can be realized. However, if the conditions I not satisfied, the Newton iterations are employed to compute the damage increment as:

$$\left(\frac{d\mathbf{Q}}{d\boldsymbol{\kappa}}\right)\delta\boldsymbol{\kappa}=-\mathbf{Q} \tag{26}$$

and the damage vector is updated as:

$$\Delta\boldsymbol{\kappa}^{(i+1)}=\Delta\boldsymbol{\kappa}^{(i)}+\delta\boldsymbol{\kappa} \tag{27}$$

The plastic potential function defines non-associative plasticity condition as:

$$\hat{\Phi}\left(\hat{\bar{\boldsymbol{\sigma}}}\right)=\left\|\hat{\bar{\mathbf{S}}}\right\|+\alpha_p\hat{\bar{I}}_1 \tag{28}$$

The plastic strain tensor increment in time step can be calculated as follows:

$$\Delta\hat{\boldsymbol{\varepsilon}}^p=\Delta\lambda\frac{\partial\hat{\Phi}}{\partial\hat{\bar{\boldsymbol{\sigma}}}} \tag{29}$$

Finally, the update of plastic strain and damage vector can be realized as:

$${}^{t+\Delta t}\boldsymbol{\varepsilon}^p={}^{t}\boldsymbol{\varepsilon}^p+\mathbf{P}\Delta\hat{\boldsymbol{\varepsilon}}^p\mathbf{P}^T \tag{30}$$

$${}^{t+\Delta t}\boldsymbol{\kappa}={}^{t}\boldsymbol{\kappa}+\Delta\boldsymbol{\kappa} \tag{31}$$

Degradation variable can be calculated for tension and compression:

$$d=1-\left(1-d_c\left(\kappa_c\right)\right)\left(1-sd_t\left(\kappa_t\right)\right) \tag{32}$$

where s is the stiffness recovery factor. The effective stress is finally:

$$\boldsymbol{\sigma}=\left(1-d\right)\bar{\boldsymbol{\sigma}} \tag{33}$$

3. Uniaxial compression and tension test of CDP model for various types of 3d elements

The numerical analyses of monotonic uniaxial compression and tension tests were performed in PAK software (Kojić et al. 1999). Pre- and post-processing of the model is performed within Simcenter Femap software (Siemens 2021). The simulations of uniaxial tests were performed for the hexahedral elements, the tetrahedral elements and hexahedral elements degenerated into the shape of tetrahedron. The element types which are used in the numerical simulations of uniaxial compression and tension tests are shown in Fig. 1.

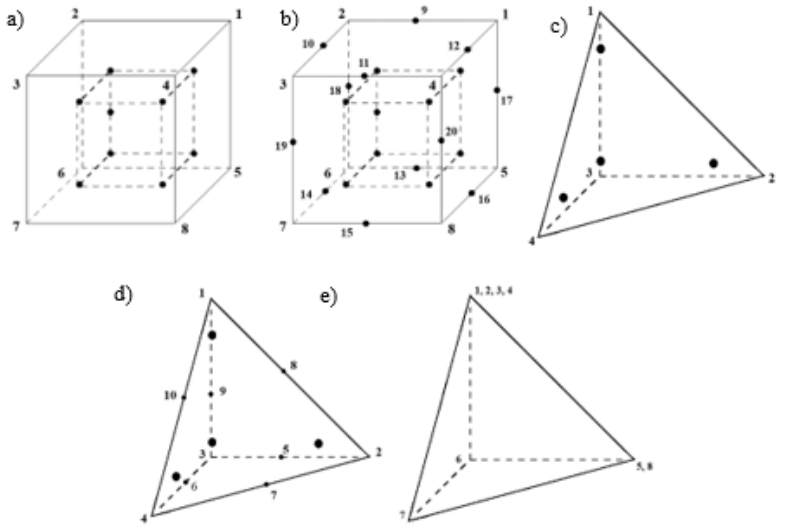

Fig. 1. Element types used for the numerical simulations. a) hexahedral element; b) hexahedral element with midside nodes c) tetrahedral element; d) tetrahedral element with midside nodes; e) hexahedral element degenerated into the shape of tetrahedron

The values of the material parameters of the CDP constitutive model, as well as the experimental data with which the comparison was made, were taken from the literature (Omidi and Lotfi 2010).

Boundary conditions are set to match the conditions of the experimental uniaxial tests of the specimen. The symmetry boundary conditions are set on the sides of the model located in symmetry planes, while the vertical displacement is constrained on the bottom side. The load is defined using prescribed displacement on the nodes located on the upper surface. The direction and value of the prescribed displacements are regulated by the load functions by which the prescribed displacements are multiplied. Schematic representation of the uniaxial tests, as well as the boundary conditions and loads are given in Fig. 2.

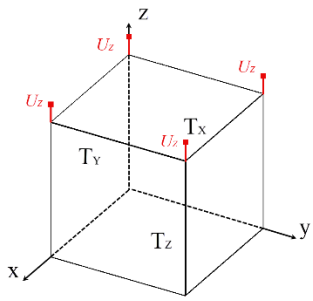

Fig. 2. Schematic representation of uniaxial tests.

The FE models are created using the different types of the finite elements: hexahedral, hexahedral with midside nodes, tetrahedral, tetrahedral with midside nodes and hexahedral elements degenerated into the shape of tetrahedron. For the hexahedral finite elements and the hexahedral elements degenerated into the shape of tetrahedron, the integration scheme 2x2x2 is considered, while for the hexahedral elements with the midside nodes, the integration scheme 3x3x3 is used. For the tetrahedral finite elements, the integration configuration with 4 integration points is considered. The FE models are shown in Fig. 3.

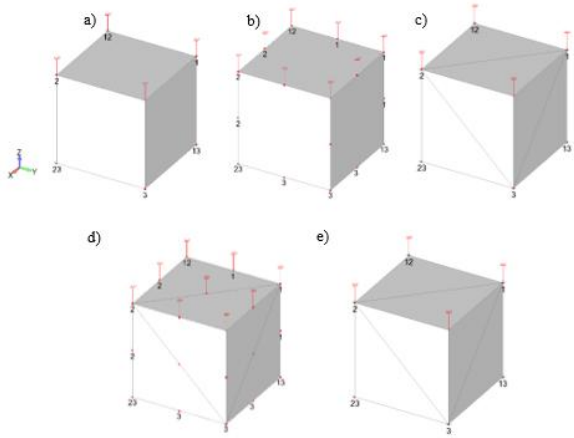

Fig. 3. The FE models created using: a) hexahedral element; b) hexahedral element with midside nodes; c) tetrahedral elements; d) tetrahedral elements with midside nodes and e) hexahedral elements degenerated into the shape of tetrahedron

All numerical analyses of the uniaxial compression and tension tests were performed in 50, 100 and 500 steps. Comparative results of all numerical analyses as well as discussion of results are given in the following section. The results are given in the form of stress – total strain and degradation – total strain dependencies.

4. Results of numerical analyses

The results of numerical simulations compared with the experimental data are given in the form of stress – total strain dependence and degradation – total strain dependence. The labels in the legends on the following figures are as follows:

- hex: hexahedral finite element with integration scheme 2x2x2;
- hex - MN: hexahedral finite element with midside nodes and integration scheme 3x3x3;
- tet: tetrahedral finite elements with 4 integration points;
- tet - MN: tetrahedral finite elements with midside nodes and 4 integration points;
- hex_deformed_in_tet: degenerate hexahedral elements in the shape of a tetrahedron.

The stress – total strain dependence for the uniaxial compression tests for 100 time steps are given in Fig. 4.

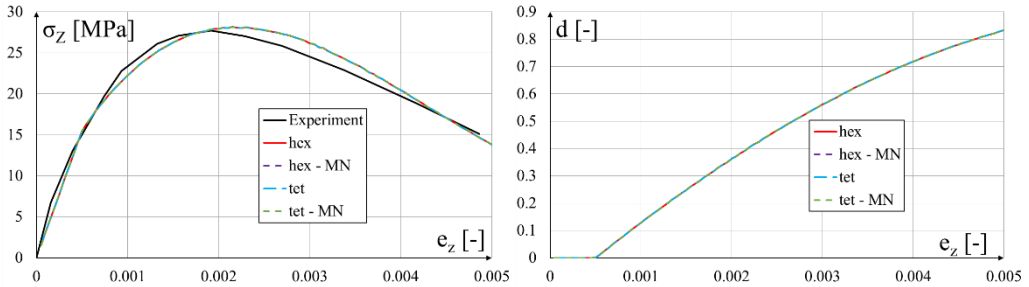

Fig. 4. Uniaxial compression test: stress – total strain (left) and degradation – total strain (right) dependence for different element types compared with experimental results – 100 steps.

Based on the Fig. 4, it can be concluded that the results of the numerical analyses of uniaxial compression tests for all types of finite elements coincide with each other. A minor deviation exists between the stress – total strain dependencies of the numerical analyses and the same dependencies of the experimental test from the literature. Also, all numerical simulations with 50 and 500 time steps for the uniaxial compression test converge and give identical solutions. The stress – total strain dependencies for the uniaxial tension tests for 100 steps are given in Fig. 5.

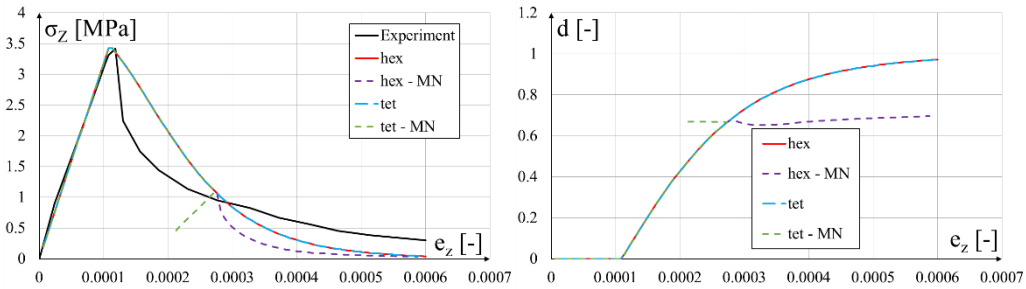

Fig. 5. Uniaxial tension test: stress – total strain (left) and degradation – total strain (right) dependence for different element types compared with experimental results – 100 steps.

The stress – total strain dependencies for uniaxial tension tests for 50 steps and increment value of 1 are given in Fig. 6.

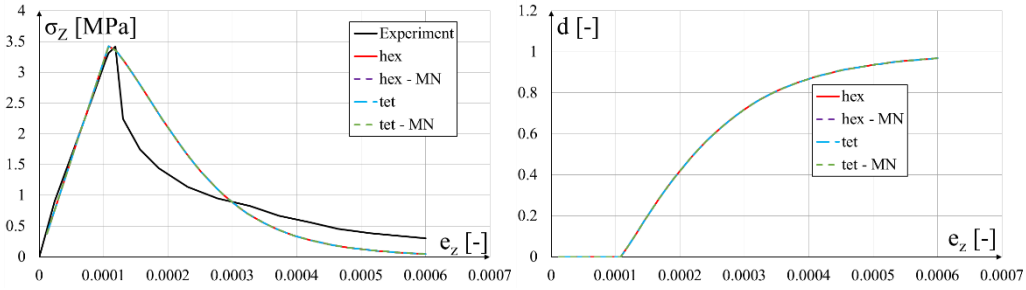

Fig. 6. Uniaxial tension test: stress – total strain (left) and degradation – total strain (right) dependence for different element types compared with experimental results – 50 steps

The stress – total strain dependencies for uniaxial tension tests for 500 steps and increment value of 1 are given in Fig. 7.

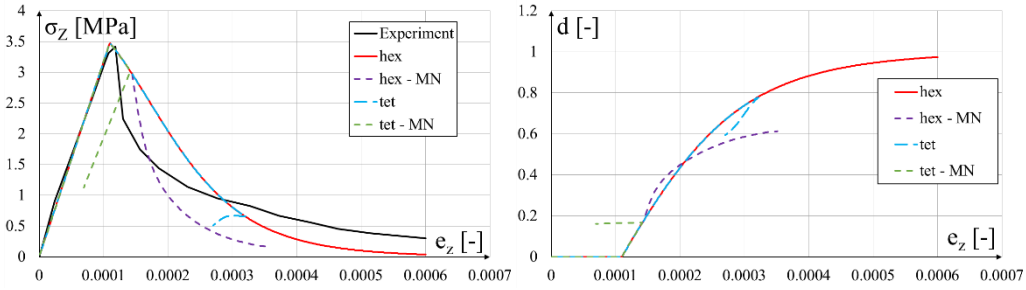

Fig. 7. Uniaxial tension test: stress – total strain (left) and degradation – total strain (right) dependence for different element types compared with experimental results – 500 steps

By observing the results of numerical analyses of uniaxial tensile tests, shown in Fig. 5 – Fig. 7, it can be concluded that the best match of the numerical results with the experimental data is for simulations with 50 time steps. For this number of time steps all calculations converge. With the increase in the number of time steps from 50 to 100, the calculation for the models with the

tetrahedral and hexahedral finite elements with midside nodes do not converge and deviate from experimental results. Also, with an increase from 100 to 500 steps, the calculation for the hexahedral element without midside nodes is the only one that converges and gives the best matches with experiment.

A comparison of the stress-total strain dependencies for the uniaxial tensile test between the model created with the tetrahedral finite elements and the degenerate hexahedral elements in the shape of a tetrahedron for 100 steps and an increment value of 1 is given in Fig. 8.

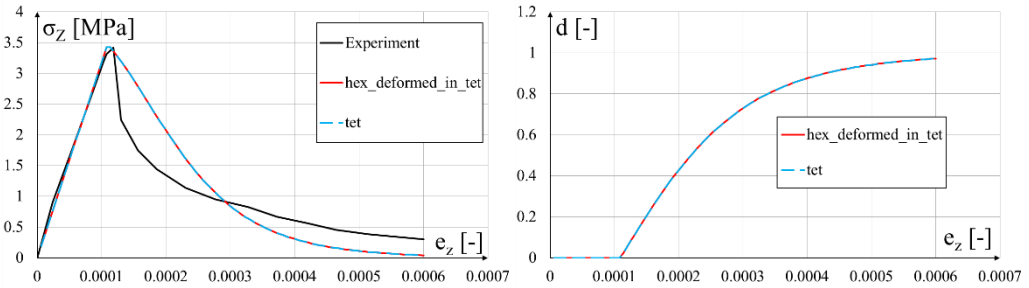

Fig. 8. Uniaxial tension test: stress – total strain (left) and degradation – total strain (right) dependence for the model created with tetrahedral finite elements and the degenerate hexahedral elements in the shape of a tetrahedron - 100 steps.

By observing the results of the numerical analyses of the uniaxial tensile tests, shown in Fig. 8, it can be concluded that the degeneracy of the hex element into a tetrahedron shape gives the same results as using the tetrahedral finite element without midside nodes.

5. Conclusions

The response of CDP constitutive model is investigated by the uniaxial compression and tension tests using various type of finite elements. The obtained results suggest that the stability of response depends on the element type, where the significant influence can be noticed for the models with and without midside nodes. Also, the influence of the various time steps size is analysed. It can be noticed that the response of CDP model is stable for the compression test for all elements and time step size. On the other side, the tension loading conditions strongly depend on the variation of element and the time step size, when the damage value increases. The time step size is also important factor, as for the relatively small increase of the external forces, the convergence is questionable, for the elements with the midside nodes.

Acknowledgements This research is supported by the Science Fund of the Republic of Serbia, #GRANT No 7475, Prediction of damage evolution in engineering structures – PROMINENT.

References

Altaee M, Kadhim M, Altayee S, Adheem A (2020). Employment of damage plasticity constitutive model for concrete members subjected to high strain-rate. 1st International Multi-Disciplinary Conference Theme: Sustainable Development and Smart Planning, Cyberspace.

Al-Zuhairi A, Al-Ahmed A, Abdulhameed A, Hanoon A (2022). Calibration of a New Concrete Damage Plasticity Theoretical Model Based on Experimental Parameters. *Civil Engineering Journal*, 8(2).

Bosro M Z M, Mohamad N, Samad A A A, Goh W I, Noranai Z, Tambichik M A, Mokhtar N, Hakim S J S (2024). Damage plasticity model for green concrete material. Kuala Lumpur, Malaysia, IOP Conf. Ser.: Earth Environ. Sci., 1347, 012075

Fedoroff A, Calonius K (2020). Using the Abaqus CDP model in impact simulations. *Journal of Structural Mechanics*, 53(3), 180-207.

Grassel P, Xenos D, Nystrom U, Rempling R, Gylltoft K (2013). CDPM2: A damage-plasticity approach to modelling the failure of concrete. *International Journal of Solids and Structures*, 50(24), 3805-3816.

Kojić M, Slavković R, Živković M, Grujović N (1998). *Metod konačnih elemenata I*. Mašinski fakultet Univerziteta u Kragujevcu, Kragujevac, Serbia.

Kojić M, Bathe K -J (2005). *Inelastic Analysis of Solids and Structures*. Springer, Berlin, Heidelberg, Germany.

Kojić M, Slavković R, Živković M, Grujović N (1999). *PAK-finite element program for linear and nonlinear structural analysis and heat transfer*. University of Kragujevac, Faculty of Mechanical Engineering. Kragujevac, Serbia

Labibzadeh M, Namjoo H (2020). Size Effects on Concrete Damaged Plasticity Model. *Cur Trends Civil & Struct Eng.*, 6(3).

Labibzadeh M, Zakeri M, Adel Shoaib A (2017). A new method for CDP input parameter identification of the ABAQUS software guaranteeing uniqueness and precision. *International Journal of Structural Integrity*, 8(2), 264-284.

Le Minh H, Khatir S, Abdel Wahab M, Cuong-Le T (2021). A concrete damage plasticity model for predicting the effects of compressive high-strength concrete under static and dynamic loads. *Journal of Building Engineering*, 44, 103239.

Lee J (1996). *Theory and implementation of plastic-damage model for concrete structures under cyclic and dynamic loading*. University of California, Berkeley, USA.

Lee J, Fenves G (1998). Plastic-Damage Model for Cyclic Loading of Concrete Structures. *Journal of Engineering Mechanics*, 124(8).

Lubliner J, Oliver J, Onate E (1989). A plastic-damage model for concrete. *International Journal of Solids and Structures*, 25(3), 299-326.

Martin O (2010). Comparison of different Constitutive Models for Concrete in ABAQUS/Explicit for Missile Impact Analyses, Netherlands: JRC-IE - Scientific and Technical Reports.

Omidi O, Lotfi V (2010). Finite Element Analysis of Concrete Structures Using Plastic - Damage Model in 3-D Implementation. *International Journal of Civil Engineering*, 8(3), 187-203.

Qasem M, Hasan M, Muhamad R, Chin C -L, Alanazi N (2025). Generalised calibration and optimization of concrete damage plasticity model for finite element simulation of cracked reinforced concrete structures. *Results in Engineering*, 25, 103905.

Rakić D, Bodić A, Milivojević N, Dunić V, Živković M (2021). Concrete damage plasticity material model parameters identification. *Journal of the Serbian Society for Computational Mechanics*, 111-122.

Siemens (2021). FEMAP User Guide - Version 2021.2: Siemens DI Software Simcenter Femap.

Sümer Y, Aktaş M (2015). Defining parameters for concrete damage plasticity model. *Challenge Journal of Structural Mechanics*, 1(3), 149-155.

Szczecina M, Winnicki A (2015). Numerical simulations of corners in RC frames using Strut-and-Tie Method and CDP model. XIII International Conference on Computational Plasticity. Fundamentals and Applications COMPLAS XIII

Talaat M, Yehia E, Mazek SA, Genidi MMM, Sherif AG (2021). Finite element analysis of RC buildings subjected to blast loading. *Ain Shams Engineering Journal*, 13(4), 101689.

Wang Q, Hou K K, Lu J, Dong Q H, Yao D P, Lu Z (2020). Study on concrete damaged plasticity model for simulating the hysteretic behavior of RC shear wall. IOP Conf. Ser.: Mater. Sci. Eng. 789 012065